JOURNAL OF BACTERIOLOGY, Oct. 1989, p. 5296–5303
0021-9193/89/105296-08$02.00/0

Vol. 171, No. 10

Structure, Surface Charge, and Self-Assembly of the S-Layer Lattice from *Bacillus coagulans* E38-66

DIETMAR PUM,* MARGIT SÁRA, AND UWE B. SLEYTR

Zentrum für Ultrastrukturforschung, Universität für Bodenkultur, und Ludwig Boltzmann-Institut für Ultrastrukturforschung, 1180 Vienna, Austria

Received 10 April 1989/Accepted 20 June 1989

In freeze-etched preparations, whole cells from *Bacillus coagulans* E38-66 exhibited an oblique S-layer lattice (a = 9.4 nm; b = 7.4 nm; γ = 80°). The three-dimensional structure of the crystalline array was characterized by optical and computer image analysis. The lattice showed two distinctly shaped types of pores. In vitro self-assembly of isolated subunits yielded flat sheets and open-ended cylinders composed of two back-to-back monolayers. Unlike whole cells, in vitro self-assembly products were capable of binding polycationized ferritin (pI, ~11). This showed that only the inner S-layer face adhering to the peptidoglycan-containing layer in whole cells was net negatively charged. S-layer monomers and/or oligomers were capable of generating a closed monolayer with oblique symmetry on poly-L-lysine-coated supports. The monolayer had a typical crazy paving appearance, with numerous crystal boundaries. The handedness of the oblique lattice and ability to bind polycationized ferritin revealed that the subunits had bound with the outer, not net negatively charged face to the poly-L-lysine-coated supports. Carbodiimide-activated carboxyl groups on either cell wall fragments or self-assembly products could covalently bind high-molecular-weight nucleophiles such as ferritin. This confirmed the location of negatively charged carboxyl groups on the outermost surface of both S-layer faces. The difference in pH optimum for carbodiimide activation indicated a preponderance of α- and β-carboxyl groups on the inner S-layer face and a preponderance of β- and γ-carboxyl groups on the outer S-layer face.

Regularly structured surface layers (S layers) represent the outermost cell envelope component in many bacteria (for recent reviews, see references 2, 8, 22, and 23). S-layer lattices which are formed of assemblies of a single protein or glycoprotein species can exhibit oblique, square, or hexagonal symmetry (9, 10, 21, 23, 25). Generally, the center-to-center spacing of the morphological units, which is a strain-specific feature, can range from 5 to 32 nm (23).

Comparative studies on S layers from numerous *Bacillus stearothermophilus* and *Desulfotomaculum nigrificans* strains revealed a considerable diversity in morphological properties, molecular weight of the protomers, and the presence of covalently attached carbohydrate residues (13, 24). However, permeability studies supported by high-resolution electron microscopy showed that S layers of all *B. stearothermophilus* strains examined possess pores larger than 3.5 nm (13, 18). In all strains, the outer face of the S-layer lattice revealed free amino and carboxyl groups but did not show the net negative surface charge (14, 17) that is characteristic for S-layer-deficient bacteria (5). A surplus of free carboxyl groups was only described for the inner S-layer face adhering to the rigid cell wall layer (14, 17, 18). These accumulated data indicate common features of functional significance for S layers of thermophilic *Bacillaceae*. For example, from identical surface net charges and the presence of free amino and carboxyl groups on the outermost S-layer surface, very similar adsorption and binding properties of whole cells can be expected. Likewise, similar pore sizes in the crystalline arrays will lead to comparable molecular-sieving properties of S layers. In other words, the observed heterogeneity of S layers at the structural level is obviously not expressed in factors influencing the behavior and survival strategies of whole cells in natural environments.

In this study, we investigated the oblique S-layer lattice from *Bacillus coagulans* E38-66 to learn more about the relatedness of S layers from strains belonging to different species but living in comparable natural habitats.

MATERIALS AND METHODS

Bacterial strain and growth conditions. *Bacillus coagulans* E38-66 was kindly provided by F. Hollaus (Österreichisches Zuckerforschungsinstitut, Fuchsenbigl, Austria). Bacteria were grown at 63°C in continuous culture under conditions given previously (24).

Cell wall preparation and self-assembly. Cell wall preparation and extraction of the S-layer protein with guanidine hydrochloride (GHCl; 5 M in 50 mM Tris hydrochloride buffer [pH 7.2]) was performed as described previously (24). For obtaining S-layer self-assembly products, GHCl extracts were dialyzed against a $CaCl_2$ solution (10 mM in distilled water) or against a KCl solution (20 mM in distilled water) for 24 h at 20°C.

Electrophoresis. Sodium dodecyl sulfate (SDS)-polyacrylamide gel electrophoresis of whole cells and cell wall fragments was done under conditions given previously (13). For molecular weight determination, the high-molecular-weight standard SDS-6H (Sigma Chemical Co.) was used.

Electron microscopy. Negative staining with uranyl acetate, ultrathin sectioning, and freeze-etching were done as described before (13). Electron microscopy was done with a Philips CM 12/STEM transmission electron microscope (TEM) with the low-dose facility and a Philips 301 TEM at 80 kV.

Image processing. Micrographs were scanned with an optical diffractometer and selected for subsequent computer image processing when several high-resolution spots were found beyond a 1/2.5 nm^{-1} threshold. Digitized data (512 by 512 pixels) were preprocessed and Fourier transformed. Amplitudes and phases of the diffraction maxima were interpolated with the use of a peak profile-fitting procedure

* Corresponding author.

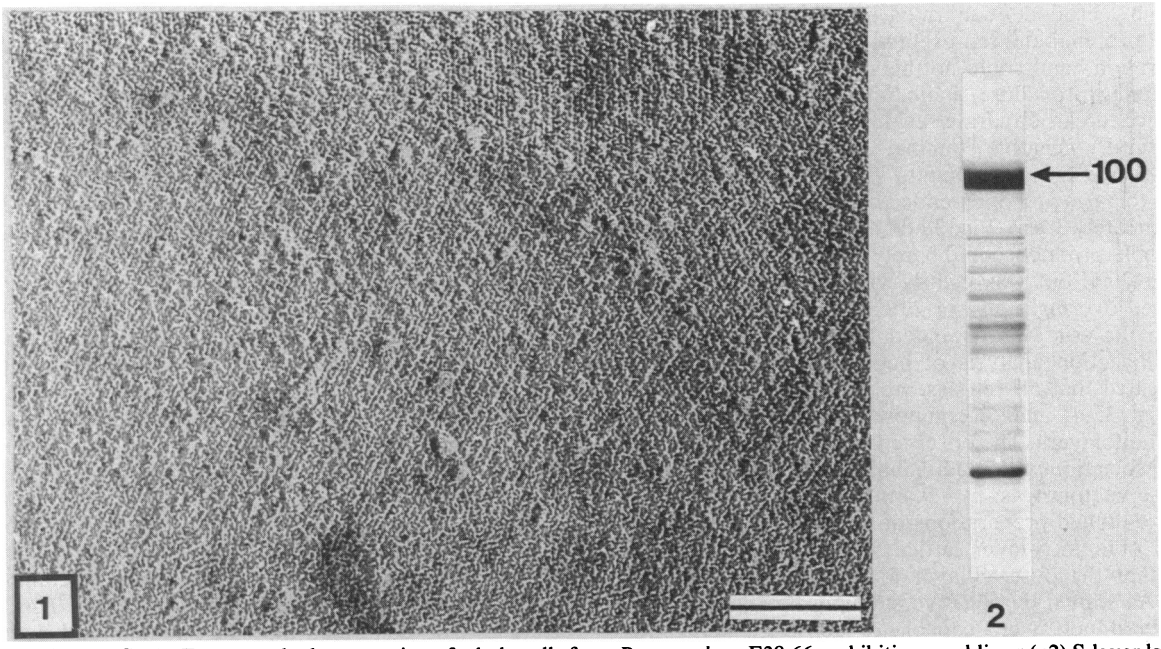

FIG. 1 and 2. FIG. 1. Freeze-etched preparation of whole cells from *B. coagulans* E38-66, exhibiting an oblique (p2) S-layer lattice with a typical crazy paving appearance. Bar, 100 nm. FIG. 2. SDS extracts of whole cells of *B. coagulans* E38-66, separated on 10% SDS gels. Arrow, 100,000-molecular-weight protein.

(11, 15). "One-sided" filtering of superimposed lattices was used to obtain single-layer reconstructions of double-layer self-assembly products. Symmetry-related pairs were complex averaged. Several tilt series with different orientations of the tilt axis against the lattice orientation were used for calculation of the three-dimensional (3D) model (8 tilt series, 120 micrographs in a tilting range of ±60°). Procedures based on the programs written at Medical Research Council, Cambridge, U.K. (1, 6), were used to obtain a set of 3D-structure factors. Backtransformation, rescaling, and thresholding of the data were done as described before (1, 16). Finally, the 3D model was represented by plotting the outlines at each level with different perspective views and a hidden line algorithm.

Labeling with PCF. Labeling of intact cells and S-layer self-assembly products with polycationized ferritin (PCF; Sigma F7879) was done as described before (17). For labeling of S layers already adsorbed to positively charged grids, the PCF preparation was dialyzed against distilled water before use.

Coating of grids with poly-L-lysine. The GHCl extract, containing approximately 2 mg of S-layer protein per ml, was dialyzed against a $CaCl_2$ solution (10 mM in distilled water) for 2 h at 20°C and subsequently stored for 20 h at 4°C. Formvar- and carbon-coated grids were glow-discharged and floated on a drop of a poly-L-lysine (Sigma P2636) solution (0.1% in distilled water) for 10 min. After excess poly-L-lysine was removed, the grids were incubated with the self-assembly suspension for 10 min to 2 h at 20°C and subsequently used for negative staining. In later studies, the self-assembly suspensions were centrifuged for 10 min at 5,400 × *g*, and the clear supernatant containing S-layer protein not assembled into supramolecular structures was used.

The protein content of the self-assembly suspension and in the clear supernatant was determined by the method of Lowry et al. (12).

Cross-linking with glutaraldehyde and covalent attachment of ferritin to carbodiimide-activated carboxyl groups. Cross-linking of whole cells, cell wall fragments, and S-layer self-assembly products with glutaraldehyde was done as described previously (17, 18). Glutaraldehyde-treated whole cells were used for PCF labeling (17). Carboxyl groups on cell wall fragments and self-assembly products were activated with EDC [1-ethyl-3,3'-(dimethylamino)propylcarbodiimide; Sigma E7750] (4, 17) at pH 3.0, 3.5, 3.8, 4.2, and 4.6 for 80 min at 20°C. After centrifugation at 20,000 × *g* for 10 min and washing of the pellets with ice-cold distilled water, the activated samples were incubated with 2 ml of a ferritin (Sigma F4503) solution (3 mg/ml of distilled water) for 18 h. For removing noncovalently bound ferritin, samples were washed with distilled water and 0.1 M phosphate buffer (pH 7.0) several times. The amount of ferritin covalently bound was calculated by subtraction of the amount detected in the supernatants of the EDC-activated samples from that detected in the supernatants of the nonactivated samples. Ferritin measurement was done in a Beckman spectrophotometer (model 25) at 280 nm.

The protein content in cell wall fragments and S-layer self-assembly suspensions was determined by the method of Lowry et al. (12) with pure S-layer protein used to construct the standard curve. The dry weight of glutaraldehyde-treated cell wall fragments was determined by drying at 115°C for 2.5 h.

RESULTS

Freeze-etched preparations from whole cells of *B. coagulans* E38-66 exhibited highly ordered patches of an oblique S-layer lattice (Fig. 1). Although numerous crystal boundaries were observed on cell poles and even on the cylindrical part of the cell (Fig. 1), the S-layer lattice completely covered the cell surface.

SDS extracts from whole cells yielded a distinct major protein band with an apparent molecular weight of 100,000 on SDS gels (Fig. 2). Cell wall preparations and pure S-layer

self-assembly products confirmed that the 100,000-molecular-weight protein band represented the S-layer protein. The S-layer protein band could not be stained by the periodate-Schiff staining procedure, indicating the absence of covalently attached carbohydrate residues.

As shown by negative staining, in vitro self-assembly of GHCl-extracted S-layer subunits yielded flat sheets with a size of up to 5 μm and open-ended cylinders with a diameter of approximately 1 μm (Fig. 3 and 4). The oblique lattice on self-assembly products could barely be seen after only 2 h of dialysis at 20°C but was clearly visible when suspensions were stored overnight at 4 or 20°C without further dialysis and when dialysis was extended to 24 h (Fig. 3 and 4). Optical diffraction analysis of negatively stained preparations revealed that all self-assembly products were double layers (Fig. 3, 4, and 5) composed of two back-to-back-oriented monolayers. The observed moiré patterns indicated random association of the individual monolayers. The length of the base vectors was: a = 9.4 nm, b = 7.4 nm; γ = 80°.

In freeze-etched preparations of native cells treated with PCF, the oblique S-layer lattice was still clearly visible, showing that the outer S-layer face is not net negatively charged. As shown by negative staining, double-layer self-assembly products were capable of densely binding PCF molecules (Fig. 6). These comparative studies clearly demonstrated that the inner S-layer faces show a net negative surface charge and are accessible to PCF molecules in double-layer self-assembly products. Thus, the constituent monolayers bind to each other through the outer, not net negatively charged faces.

Thin-section preparations confirmed the results from optical diffraction analysis that all self-assembly products are double layers (not shown). The constituent monolayers were 4.5 nm thick, which is in accord with data from 3D reconstruction. The 3D model is shown in Fig. 7 and 8. Each morphological unit was composed of a dimer. The bulk of the protein was located around the central twofold axis and displayed a characteristic handedness. Subunits along the long base vector were connected by two arms, yielding an S-shaped pore in projection (Fig. 7a and 8a). Along the short base vector and the diagonal, only one contact region with an ovoid pore can be seen. In the direction perpendicular to the S-layer plane, the pores seemed to be twisted cylindrical channels rather than aperturelike openings (Fig. 7b and c, 8b and c). Derived from the dimensions of the unit cell, the size of the ovoid pore was calculated to be in the range of 2.8 by 3.2 nm, and the S-shaped pore was approximately 2 by 4.5 nm. The 3D model further revealed that the outer S-layer face (Fig. 7a to c) was smoother than the inner S-layer face (Fig. 8a to c).

As shown by negative staining, individual sheetlike and cylindrical self-assembly products could adsorb to glow-discharged grids floated on self-assembly suspensions for 10 to 60 min. By contrast, a closed regularly structured layer revealing the characteristic oblique lattice was detected when poly-L-lysine-coated grids were floated on self-assembly suspensions for 1 h (Fig. 9 and 10a). The regularly structured layer had a crazy paving appearance, with numerous crystal boundaries (Fig. 9), but all the randomly oriented crystallites revealed the same handedness (Fig. 9 and 10a). Optical diffraction analysis showed that the oblique lattice represented a monolayer. Comparison of the handedness of the crystallites with that observed in the oblique lattice on intact cells revealed that the S-layer subunits had bound with the outer face to the poly-L-lysine-coated supports. An incubation time of only 10 min led to the formation of isolated crystallites but not to a closed monolayer.

When S-layer self-assembly products obtained by dialysis of GHCl extracts were sedimented by centrifugation, a clear supernatant containing 80% of the total S-layer protein was obtained, showing that only 20% of the subunits had been incorporated into sheetlike or cylindrical self-assembly products. Since incubation of the clear supernatant with poly-L-lysine-coated grids also yielded a closed regularly structured monolayer, it seems that monolayers were generated by crystal growth of initially adsorbed monomers, oligomers, or small crystallites. This would also explain the random orientation of crystallites and the zig-zag crystal boundaries (Fig. 9). Furthermore, it was demonstrated by negative staining that monolayers generated on positively charged grids were capable of binding PCF (Fig. 10b). Both the lattice orientation and crystal boundaries could be recognized in such labeled preparations (Fig. 10b). This labeling characteristic confirmed that the subunits had bound with the outer face to poly-L-lysine-coated grids. A survey on the orientation of the S-layer lattice on whole cells, in double-layer self-assembly products, and on poly-L-lysine-coated supports is given in Fig. 11.

Thin-section preparations of native and PCF-treated cell wall fragments revealed that both faces of the peptidoglycan-containing layer were covered with an S layer in the natural orientation. Unlike native S layers, the outer face of glutaraldehyde-treated S-layer material was capable of densely binding PCF (not shown). The net negative surface charge was attributed to the loss of the free amino groups by reaction with glutaraldehyde and to the presence of free carboxyl groups.

With glutaraldehyde-treated cell wall fragments, carboxyl groups on only the outer S-layer face would be capable of covalently binding high-molecular-weight nucleophiles after carbodiimide activation. Ferritin (pI, 4.3; molecular weight, 440,000; molecular size, 12 nm) was found to be an optimal nucleophile for proving this hypothesis, since it did not show any unspecific adsorption to S layers.

When carbodiimide activation was performed at pH 4.2, 46 μg of ferritin was covalently bound per mg (wet weight) of pellet. Since the S-layer protein constitutes 72% of cell wall fragments, possessing a dry weight of 7%, 940 μg of ferritin was bound per mg of S-layer protein. Thus, 1 ferritin molecule was covalently attached per 4 to 5 S-layer monomers. Considering the molecular weight of ferritin (440,000) and that of the S-layer protein (100,000), the ratio between S-layer subunits and immobilized ferritin molecules reflects the dense arrangement of ferritin molecules. The pH optimum for carbodiimide activation of carboxyl groups on the outer S-layer face was found to be between 3.8 and 4.6. Approximately 70 and 90% of ferritin was bound when activation was performed at pH 3.0 and 3.5, respectively. For covalent attachment of ferritin to carbodiimide-activated carboxyl groups on the inner S-layer face, double-layer

FIG. 3–6. FIG. 3. Negative staining of double-layer sheetlike S-layer self-assembly products. Bar, 100 nm. FIG. 4. Open-ended cylindrical S-layer self-assembly product. Bar, 100 nm. FIG. 5. Diffraction pattern from double-layer sheetlike S-layer self-assembly products. FIG. 6. Negative staining of a sheetlike S-layer self-assembly product, labeled with PCF. Arrows indicate one of the two base vectors in the individual monolayers. Bar, 100 nm.

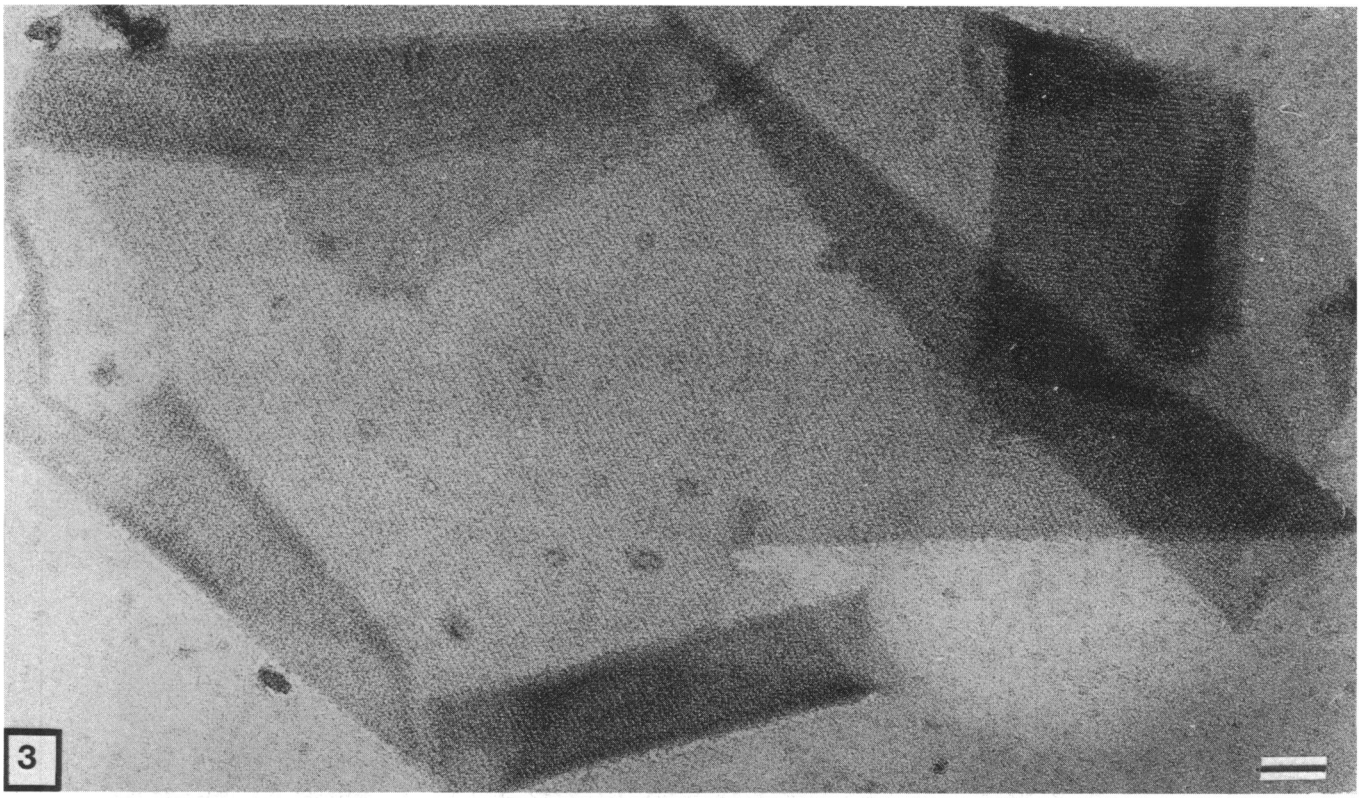
3

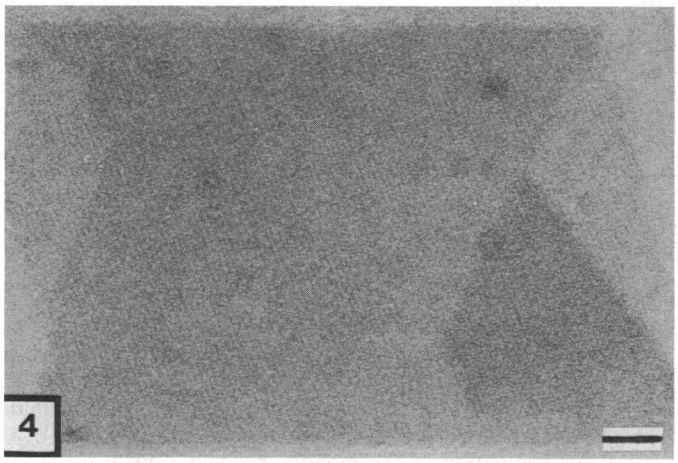
4

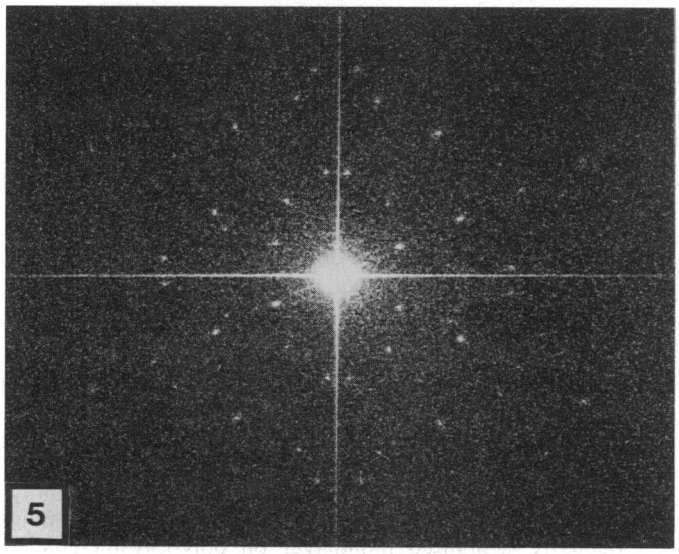
5

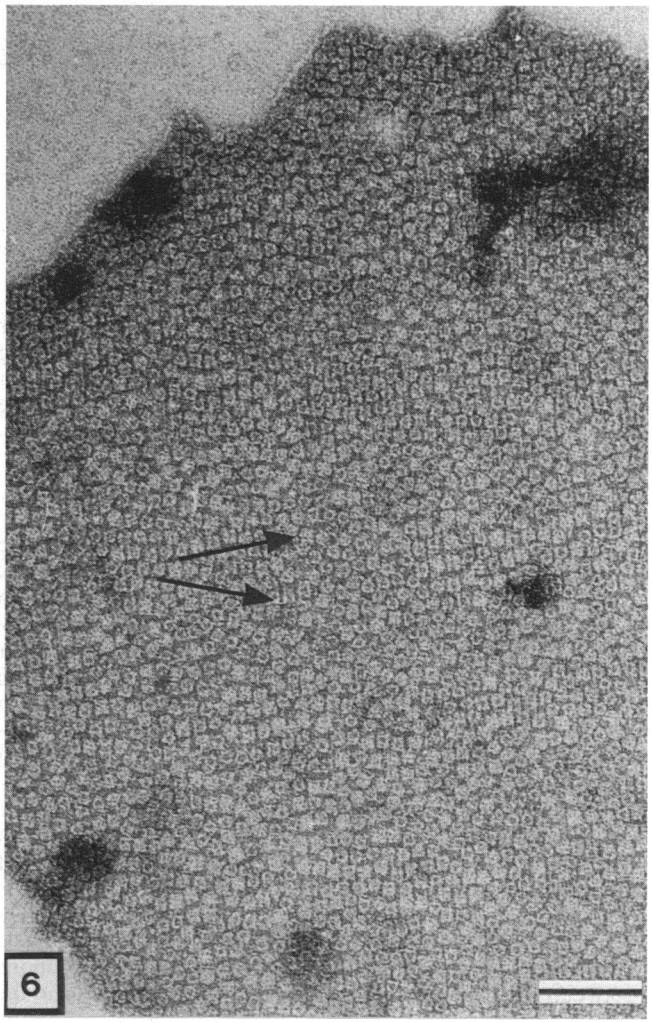
6

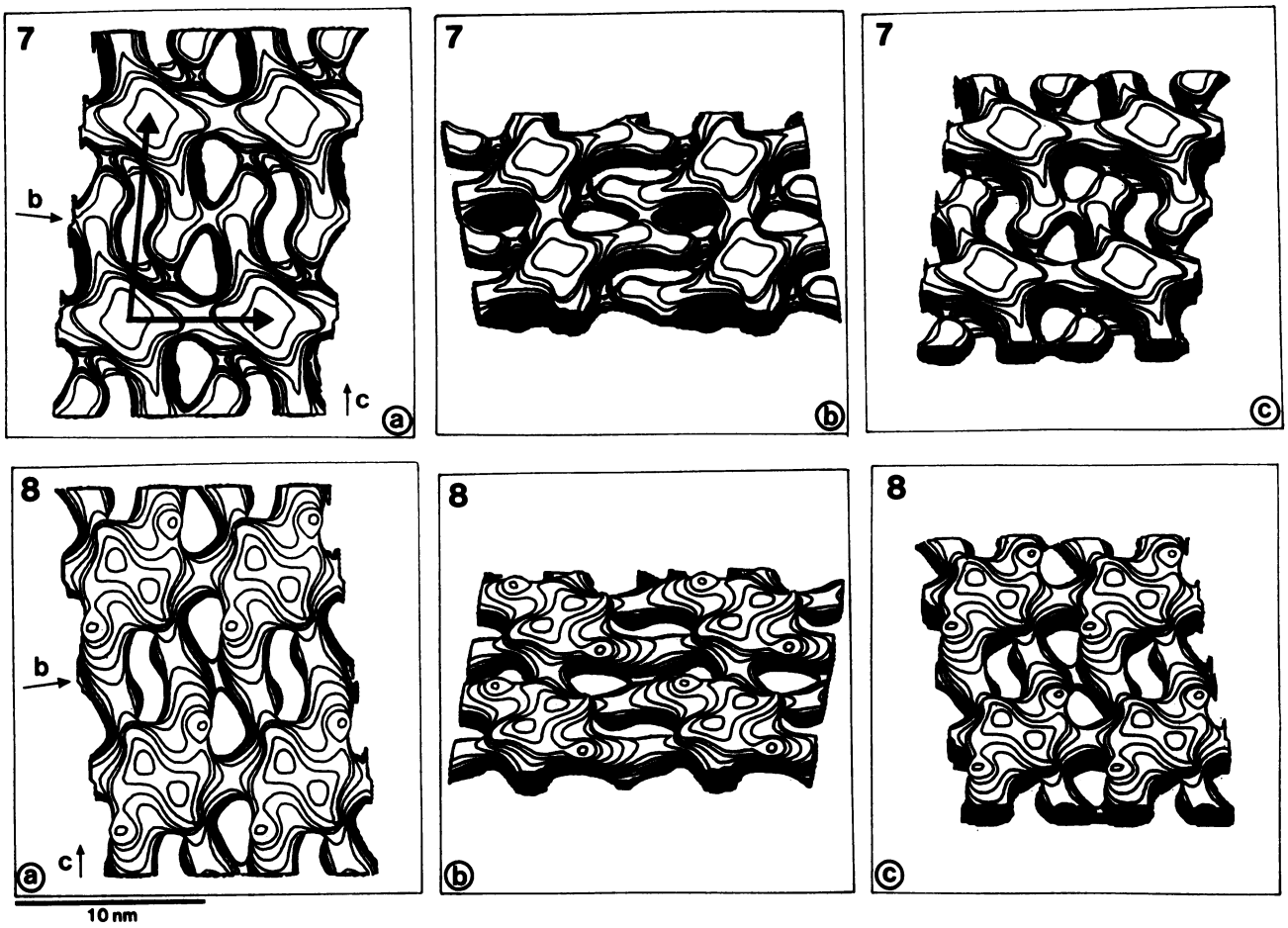

FIG. 7 and 8. FIG. 7. Image reconstruction of the oblique S-layer lattice from *B. coagulans* E38-66. (a) Top view of the outer face; (b and c) views of structure in panel a tilted 45°. FIG. 8. (a) Top view of the inner S-layer face; (b and c) views of structure in panel a tilted 45°.

self-assembly products were used. The pH optimum for carbodiimide activation was found to be 3.0, whereas 850 μg of ferritin could be immobilized per mg of S-layer protein. At pH 3.8 to 4.6, only 490 μg of ferritin could be bound per mg of S-layer protein, which corresponds to 58% of the maximum.

DISCUSSION

Like those of S layers from many other thermophilic organisms (14, 17, 18), the oblique S-layer lattices from *B. coagulans* E38-66 and *B. stearothermophilus* NRS 2004/3a (14) exhibited considerable asymmetry in the charge distribution on the outer and inner S-layer face. Only the inner S-layer faces showed a net negative surface charge, which seems to be required for establishing salt bridges between the protomers and the net negatively charged murine sacculus (3, 19, 21). Unlike *B. stearothermophilus* NRS 2004/3a (14) and *Aquaspirillum* (*Spirillum*) *putridiconchylium* (3a, 3b), for whose S layers the first detailed descriptions on the structure and assembly of oblique lattices have been given, the S-layer lattice from *B. coagulans* E38-66 did not exhibit a good long-range order on the cylindrical part of the cell (Fig. 1). The typical crazy paving appearance reflects inhibited recrystallization of S-layer protomers (19, 20). The lower mobility may be explained by stronger interactions between adjacent subunits or between the monomers and the underlying rigid cell wall layer (20).

Double-layer self-assembly products from both oblique lattices were composed of two back-to-back monolayers. Contrary to double-layer self-assembly products from *B. stearothermophilus* NRS 2004/3a, in which five well-defined superposition types of monolayers were observed (14), a random association of the monolayers was typical for self-assembly products of *B. coagulans* E38-66. Double-layer self-assembly products from *B. stearothermophilus* NRS 2004/3a were only obtained in the presence of bivalent cations and could not be labeled with PCF (14), indicating that the monolayers were oriented to each other with the inner, net negatively charged faces. It seems that bivalent cations were required for generating salt bridges between carboxyl groups exposed on the inner S-layer faces. Furthermore, the five well-defined superposition types may reflect the accurate position of free carboxyl groups on the S-layer subunits, further capable of generating relatively strong noncovalent bonds. By contrast, bivalent cations were not necessary for double-layer formation in self-assembly products from *B. coagulans* E38-66. The monolayers were oriented to each other with the outer, not net negatively charged S-layer faces. This suggests that mechanisms other than salt bridges, presumably hydrophobic interactions, are responsible for monolayer association.

The S-layer protein not incorporated into self-assembly products from *B. coagulans* E38-66 was capable of forming a regularly structured monolayer on poly-L-lysine-coated

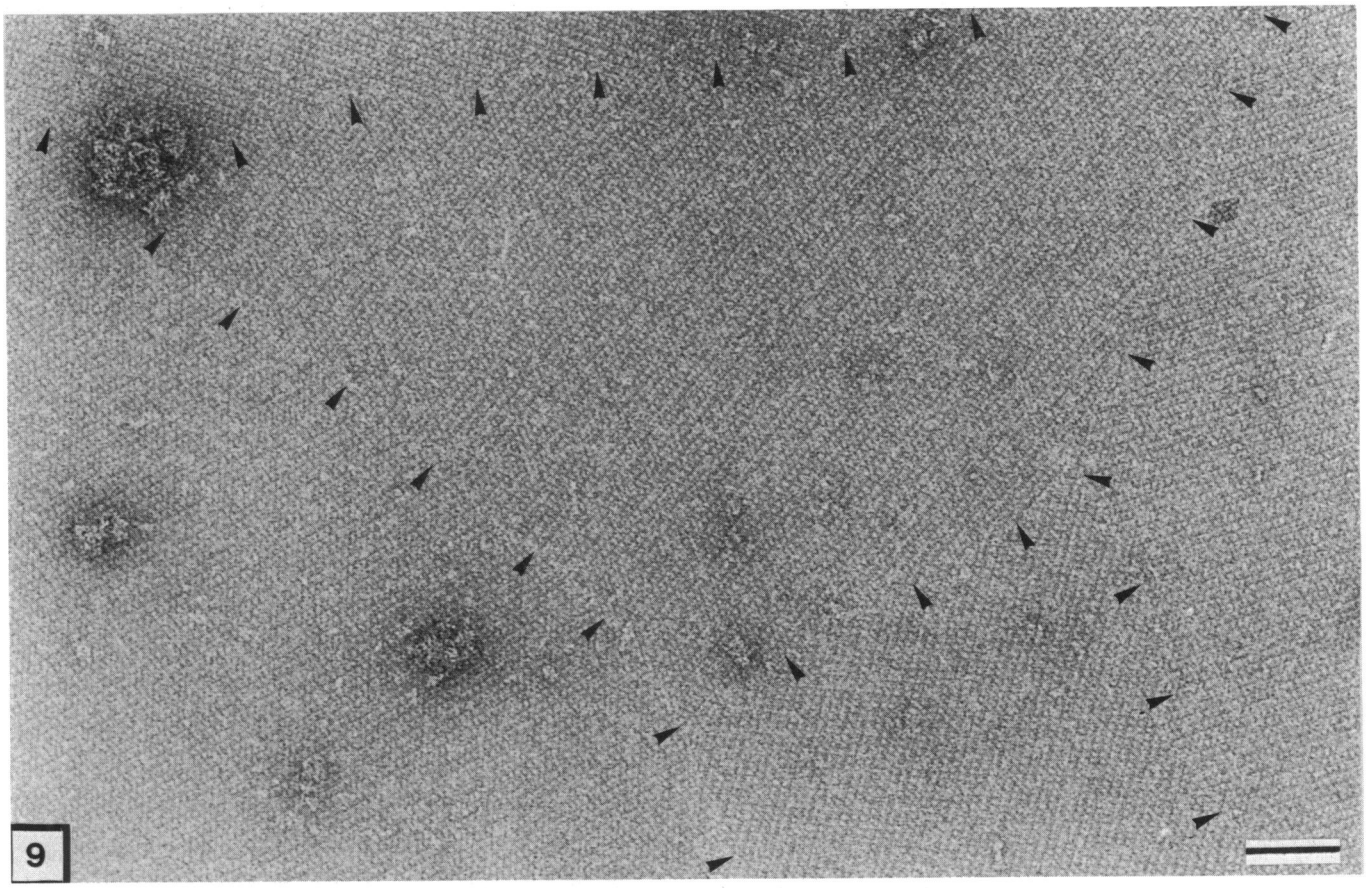

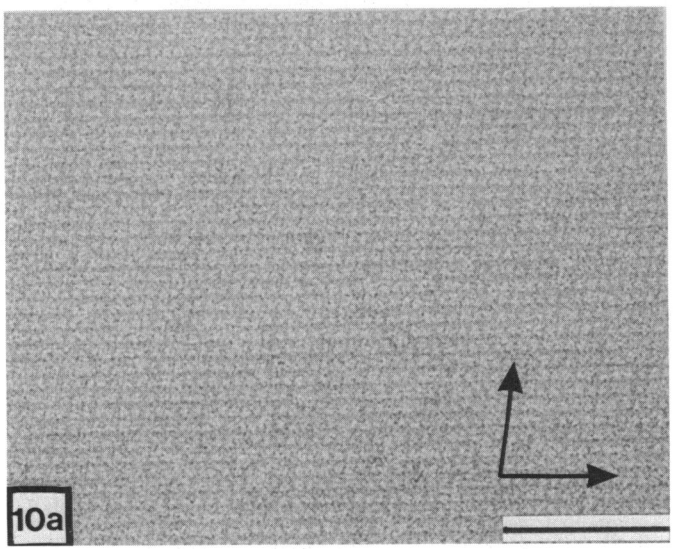

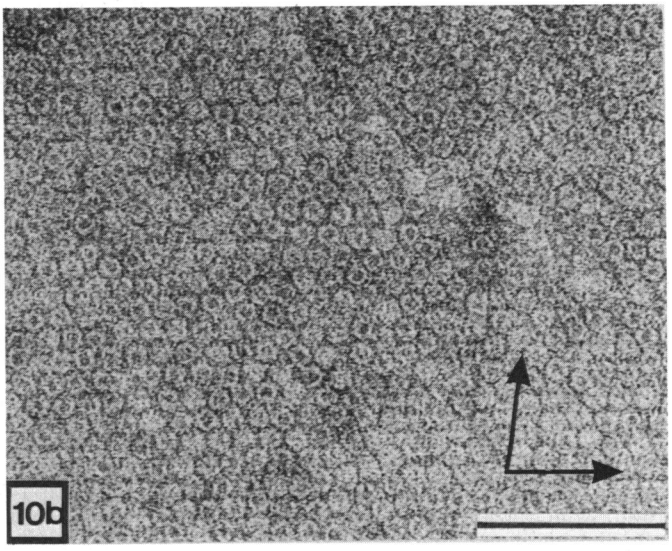

FIG. 9 and 10. FIG. 9. Negative staining of an S-layer monolayer generated on poly-L-lysine-coated grids. The monolayer reveals numerous crystal boundaries, indicated by the small arrows. Bar, 100 nm. FIG. 10. Negative staining of an S-layer monolayer generated on poly-L-lysine-coated grids, (a) before and (b) after labeling with PCF. Arrows show the base vectors of the oblique lattice. Bars, 100 nm.

surfaces. Although not expected, the protomers adhered with their outer, not net negatively charged face to the positively charged supports (Fig. 11). Surfaces pretreated with alcian blue, which is also a positively charged but small molecule, were not as suitable as poly-L-lysine in inducing crystallization of S-layer subunits. Since poly-L-lysine has a hydrophobic portion and S-layer subunits show the same orientation on poly-L-lysine-coated surfaces as in self-assembly products, it seems that the outer S-layer face is capable of creating relatively stable hydrophobic bonds. If incubation of dialyzed GHCl extracts with poly-L-lysine-coated grids was done for longer than 1 h, double-layer and even multilayer products were generated. This observation revealed that the inner net negatively charged S-layer faces also have a certain tendency to bind to each other. However, interactions between outer S-layer faces seem to be favored,

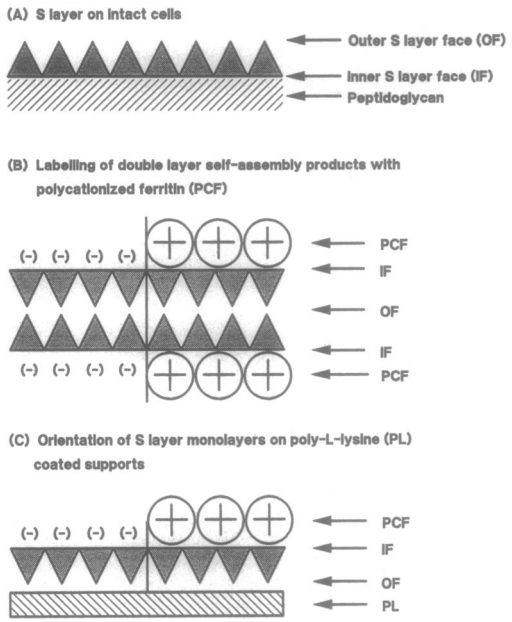

FIG. 11. Schematic drawing showing the orientation of S-layers (A) on whole cells, (B) in double-layer self-assembly products, and (C) on poly-L-lysine-coated supports. (A) The outer S-layer face (OF) exposed on whole cells is not net negatively charged. (B) The inner S-layer face (IF), which is net negatively charged (−) and accessible in double-layer self-assembly products, is capable of binding PCF. (C) Subunits bind with the outer face to poly-L-lysine-coated (net positively charged) supports.

which is contrary to the observation for the oblique S-layer lattice from *B. stearothermophilus* NRS 2004/3a.

Carboxyl groups were found to be exposed on the outermost surface of both S-layer faces from *B. coagulans* E38-66. Carbodiimide activation is usually more successful if carboxyl groups are protonated (4). Thus, the pH optimum for carbodiimide activation indicated a preponderance of α- and β-carboxyl groups on the inner S-layer face, whereas β-carboxyl groups from aspartic acid residues and γ-carboxyl groups from glutamic acid possessing higher pK values seem to be exposed on the outer S-layer face. As recently reviewed (7), S-layer proteins have more than half of their negatively charged amino acids in the last third of the polypeptide chain. Both the surplus of negative charges and the lower pH optimum for carbodiimide activation of carboxyl groups indicate that the C-terminus of the polypeptide chain is located on the inner S-layer face. Thus, the anisotropy of this extremely thin S-layer lattice is related to topographical properties as well as to the charge distribution, which will lead to a potential gradient across this anisotropic membrane.

Concerning the biological significance of the S-layer lattice from *B. coagulans* E38-66, no specific functional concept has been derived so far. From analysis of double layers, it can be concluded that the outer S-layer faces have the potential to adhere to each other. On the other hand, intact cells do not exhibit such a tendency for aggregation in vivo. This may be explained by the fact that in comparison to flat sheets, rod-shaped cells have a significantly smaller adjoining area in common, probably leading to insufficient bonding strengths.

The pore size derived from high-resolution electron microscopical studies is similar to that for other thermophilic *Bacillaceae* (13, 14, 18, 23) and reveals that these S layers will not function as selective molecular sieves for lytic hostile macromolecules such as muramidases. Nevertheless, despite the structural and chemical differences revealed so far at least among S layers of different thermophilic *Bacillaceae*, characteristic common features such as similar pore sizes and surface net charges appear to emerge.

ACKNOWLEDGMENTS

Part of this work was supported by grants from the Fonds zur Förderung der Wissenschaftlichen Forschung in Österreich and the Bundesministerium für Wissenschaft und Forschung.

LITERATURE CITED

1. **Amos, L., R. Henderson, and P. N. T. Unwin.** 1982. Three-dimensional structure determination by electron microscopy of two-dimensional crystals. Prog. Biophys. Mol. Biol. **39**:183–231.
2. **Baumeister, W., and H. Engelhardt.** 1987. Three-dimensional structure of bacterial surface layers, p. 109–154. *In* J. R. Harris and R. W. Horne (ed.), Electron microscopy of proteins, vol. 6: membraneous structure. Academic Press, Inc. (London), Ltd., London.
3. **Beveridge, T. J.** 1981. Ultrastructure, chemistry and function of the bacterial wall. Int. Rev. Cytol. **72**:229–317.

3a. **Beveridge, T. J., and R. G. E. Murray.** 1974. Superficial macromolecular arrays on the cell wall of *Spirillum putridiconchylium*. J. Bacteriol. **119**:1019–1038.

3b. **Beveridge, T. J., and R. G. E. Murray.** 1976. Reassembly *in vitro* of the superficial cell wall components of *Spirillum putridiconchylium*. J. Ultrastruct. Res. **55**:105–118.

4. **Carraway, K. L., and D. E. Koshland, Jr.** 1972. Carbodiimide modification of proteins. Methods Enzymol. **25**:616–623.
5. **Costerton, J. W., T. J. Marrie, and K. J. Cheng.** 1985. Phenomena of bacterial adhesion, p. 3–43. *In* D. C. Savage and M. Fletcher (ed.), Bacterial adhesion: mechanism and physiological significance. Plenum Publishing Corp., New York.
6. **Deatherage, J. F., K. A. Taylor, and L. A. Amos.** 1983. Three-dimensional arrangement of the cell wall of *Sulfolobus acidocaldarius*. J. Mol. Biol. **167**:832–852.
7. **Hovmöller, S., A. Sjögren, and D. N. Wang.** 1988. The structure of crystalline bacterial cell surface layers. Prog. Biophys. Mol. Biol. **51**:131–163.
8. **Kandler, O., and H. König.** 1985. Cell envelopes of archaebacteria, p. 413–457. *In* C. R. Woese and R. S. Wolfe (ed.), The bacteria, vol. 8: Archaebacteria. Academic Press, Inc., New York.
9. **Koval, S. F.** 1988. Paracrystalline protein surface arrays on bacteria. Can. J. Microbiol. **34**:407–414.
10. **Koval, S. F., and R. G. E. Murray.** 1986. The superficial protein arrays on bacteria. Microbiol. Sci. **3**:357–361.
11. **Kübler, O.** 1980. Unified processing for periodic and nonperiodic specimens. J. Microsc. Spectrosc. Electron. **5**:561–575.
12. **Lowry, O. H., N. J. Rosebrough, A. L. Farr, and R. J. Randall.** 1951. Protein measurement with the Folin phenol reagent. J. Biol. Chem. **193**:265–275.
13. **Messner, P., F. Hollaus, and U. B. Sleytr.** 1984. Paracrystalline cell wall surface layers of different *Bacillus stearothermophilus* strains. Int. J. Syst. Bacteriol. **34**:202–210.
14. **Messner, P., D. Pum, and U. B. Sleytr.** 1986. Characterization of the ultrastructure and the self-assembly of the surface layer (S layer) of *Bacillus stearothermophilus* strain NRS2004/3a. J. Ultrastruct. Mol. Struct. Res. **97**:73–88.
15. **Roberts, K., P. J. Shaw, and G. J. Hills.** 1981. High-resolution electron microscopy of glycoproteins: the crystalline cell wall of *Lobomas*. Appendix: P. J. Shaw. A peak profile analysis procedure for extracting unit cell transform data from the Fourier transforms of periodic arrays. J. Cell Sci. **51**:295–321.
16. **Saxton, W. O., and W. Baumeister.** 1984. Three-dimensional reconstruction of imperfect two-dimensional crystals. Ultrami-

croscopy **13**:57–70.
17. **Sára, M., and U. B. Sleytr.** 1987. Charge distribution on the S layer of *Bacillus stearothermophilus* NRS1536/3c and importance of charged groups for morphogenesis and function. J. Bacteriol. **169**:2804–2809.
18. **Sára, M., and U. B. Sleytr.** 1987. Molecular sieving through S layers of *Bacillus stearothermophilus* strains. J. Bacteriol. **169**: 4092–4098.
19. **Sleytr, U. B.** 1978. Regular arrays of macromolecules on bacterial cell walls: structure, chemistry, assembly, and function. Int. Rev. Cytol. **53**:1–64.
20. **Sleytr, U. B., and A. M. Glauert.** 1975. Analysis of regular arrays of subunits on bacterial surfaces; evidence for a dynamic process of assembly. J. Ultrastruct. Res. **50**:103–116.
21. **Sleytr, U. B., and P. Messner.** 1983. Crystalline surface layers on bacteria. Annu. Rev. Microbiol. **37**:311–339.
22. **Sleytr, U. B., and P. Messner.** 1988. Crystalline surface layers in procaryotes. J. Bacteriol. **170**:2891–2897.
23. **Sleytr, U. B., P. Messner, D. Pum, and M. Sára.** 1988. Crystalline bacterial cell surface layers. Springer-Verlag, Berlin.
24. **Sleytr, U. B., M. Sára, Z. Küpcü, and P. Messner.** 1986. Structural and chemical characterization of S layers of selected strains of *Bacillus stearothermophilus* and *Desulfotomaculum nigrificans*. Arch. Microbiol. **146**:19–24.
25. **Smit, J.** 1986. Protein surface layers of bacteria, p. 343–376. *In* M. Inouye (ed.), Bacterial outer membranes as model systems. John Wiley & Sons, Inc., New York.